Effects of Geometry and Orientation on Laminar Natural Convection from Isothermal Bodies

S. Lee,* M. M. Yovanovich,† and K. Jafarpur‡
University of Waterloo, Waterloo, Ontario, Canada

The effects of body shape and orientation on laminar natural convection heat transfer from isothermal, two-dimensional, and axisymmetric bodies are investigated. A new form of the body-gravity function is presented and its behavior is examined for various body shapes and orientations. The square root of the total surface area is obtained from the analysis as the charateristic body length. A definition of the aspect ratio is introduced, which can be used consistently for both two-dimensional and axisymmetric bodies. The resulting body-gravity function is observed to be weakly dependent on geometry and orientation of the bodies for a range of the aspect ratio from approximately 0.2 to 5, over which the body-gravity function resulted in a good agreement with values obtained from the existing experimental data.

Nomenclature

A = total surface area
$\tilde{A}$ = fraction of sectional area over A
$\mathcal{A}$ = local surface area
a = vertical axis of spheroid or ellipse
B = correlation constant
b = horizontal axis of spheroid or ellipse
C = laminar heat transfer coefficient
D = diameter of sphere or circular cylinder
e = measure of eccentricity defined by Eq. (30)
$F(Pr)$ = Prandtl number function
F_∞ = Prandtl number function as $Pr \to \infty$
g = gravitational acceleration
$G_{\mathcal{L}}$ = body-gravity function based on $\mathcal{L}$
H = vertical height of the body
h = heat transfer coefficient
I_1, I_2 = integrals defined by Eqs. (29) and (33)
$\mathcal{I}_1, \mathcal{I}_2$ = integrals defined by Eqs. (39) and (40)
k = thermal conductivity of fluid
L = length of the body
$\mathcal{L}$ = characteristic length of the body
L_c = classical characteristic length
m,n = correlation parameters
$Nu_{\mathcal{L}}$ = area-mean Nusselt number $h\mathcal{L}/k$
Nu^0 = diffusive limit Nusselt number as Ra $\to$ 0
P = local perimeter of the body
$P_{\max}$ = maximum perimeter of the body
Pr = Prandtl number, ν/α
r = dimensionless local horizontal radius
$Ra_{\mathcal{L}}$ = Rayleigh number, $g\beta(T_0 - T_f)\mathcal{L}^3/\alpha\nu$
T_0 = uniform surface temperature
T_f = fluid temperature remote from the body
u = dimensionless local velocity x direction
v = dimensionless local velocity in y direction
x = dimensionless coordinate parallel to the flow stream
y = dimensionless coordinate outward normal from surface
α = thermal diffusivity of fluid
β = thermal expansion coefficient
γ = aspect ratio defined by Eq. (24)
ϵ = measure of eccentricity, $\epsilon^2 = -e^2$
θ = angle between outward normal and gravity vector
ν = kinematic viscosity
Φ = dimensionless temperature, $(T - T_f)/(T_0 - T_f)$
ψ = half-apex angle of cone

Subscripts

DC = vertical double cone base-to-base
ED = vertical elliptic disk
HC = horizontal cylinder
SC = vertical single cone
SP = spheroid
VC = vertical cylinder

Presented as Paper 89-1662 of the AIAA 24th Thermophysics Conference, Buffalo, NY, June 12-14, 1989; received July 5, 1989; revision received Feb. 7, 1990.

*Research Assistant Professor of Mechanical Engineering. Member AIAA.

†Professor of Mechanical and Electrical Engineering. Associate Fellow AIAA.

‡Graduate Student, Department of Mechanical Engineering.

Introduction

LAMINAR natural convection heat transfer from isothermal bodies of various shapes and different orientations with regard to the gravity vector has been the subject of numerous investigations over the past several decades. Analytical, numerical, and experimental results are reported for the area-mean Nusselt number Nu as a function of the Rayleigh Ra and Prandtl Pr numbers for a given body shape, each with a choice of the characteristic length used in the definitions of the Nusselt and Rayleigh numbers. The characteristic length represents a physical dimension that may be chosen from several possible length scales associated with a specific body shape under investigation. Some conventional choices for the characteristic length include the diameter, the major or minor axis, a combination of the semiaxes, and the streamwise length of the body.

Although such and any other choices are sufficient in evaluating the heat transfer coefficient for given body shapes, they appear to be somewhat arbitrary and, in some cases, irrelevant representations of the length scales that are participating in the thermal/fluid mechanism driving the heat transfer phenomena. The magnitude of the reported Nusselt numbers, at a fixed value of the Rayleigh number, varies considerably not only from one shape to another but also for different choices of characteristic length. As a result, when a body of different shape is encountered, it is often difficult to estimate the value of the heat transfer coefficient from the existing relationships. Much needed attention was recently given by some researchers[1-6] who examined existing and new choices of the characteristic length in an attempt to bring together the Nu vs Ra plots for external natural convection heat and mass transfer from various body shapes and different orientations.

Convective heat transfer from an isothermal body to a surrounding fluid is a surface phenomenon. It is, therefore, reasonable to anticipate that a definition of the characteristic body length should be related to the surface area of the body.

In this study, a new form of the body-gravity function, which describes the Nu dependency on the body shape and its orientation with respect to the gravity vector is introduced. The function is obtained based on the thin boundary-layer analysis, and the square root of the total surface area of the body $\sqrt{A}$ is found to be the proper choice for the characteristic length by examining the new body-gravity function for various body shapes and different orientations. This characteristic length was first proposed by Yovanovich,[4-6] who successfully demonstrated its superiority to the classical body lengths in bringing together Nu vs Ra plots using published heat transfer results.

Background Considerations

Numerous analytical and empirical expressions are available in the literature for predicting natural convection heat transfer from isothermal bodies of various shapes and orientations to an extensive, quiescent fluid that is maintained at uniform temperature. The earliest and perhaps the simplest expression has the form

$$Nu = CRa^m \tag{1}$$

This simple expression is found to be adequate[5,6] for Rayleigh numbers of the order of 10^5 to 10^8, which correspond to the laminar boundary-layer flow regime.

As the Rayleigh number becomes smaller, however, the effect of thermal diffusion becomes significant, and the above form of equations begins to fail by underpredicting the data. In an attempt to improve the prediction in the small Rayleigh number range, other forms of expressions were considered that include

$$Nu = B + CRa^m \tag{2}$$

and the one introduced by Churchill and Chu[7] in the following blended manner:

$$Nu = [B^n + (CRa^m)^n]^{1/n} \tag{3}$$

where m is set to be 1/4 based on the theoretical boundary-layer analysis. The empirical constant n is found by a best fit to a given set of data and it can range from 1 to 15, depend-ing on the body shape and its orientation.[8,9] Values of B may be determined either by means of a data fitting technique or by considering the pure diffusion heat transfer that corresponds to $Ra \to 0$. The parameter C is, in general, dependent on Pr, m, and n values, and on the characteristic body length $\mathcal{L}$ used in defining Nu and Ra.

With a choice of the characteristic length and parametric values obtained from either analytical or experimental results, the above expressions were used with success to correlate data for various body shapes in different fluids. Unfortunately, the reported values of the parameters vary significantly between body shapes, and the characteristic length is often arbitrarily chosen prior to the analysis. No theoretical or analytical basis is available in most studies to support a particular choice of the characteristic body length and to predict values of the parameters that are necessary in estimating heat transfer from a body of different shape or orientation.

In view of predicting the heat transfer characteristics of different body shapes from available data, many researchers observed an important role of the characteristic body length. With a proper choice of the characteristic body length, the scatter in the Nusselt number may be reduced over a wide range of body shapes and aspect ratios. Many different characteristic lengths were proposed in the past and they are summarized by Yovanovich.[4] In particular, Yovanovich[6] proposed the square root of the body surface area as the characteristic length and then subsequently developed a correlation equation of the form given by Eq. (2):

$$Nu_{\sqrt{A}} = Nu^0_{\sqrt{A}} + C_{\sqrt{A}} Ra^{1/4}_{\sqrt{A}} \tag{4}$$

for $0 \le Ra_{\sqrt{A}} < 10^8$. The subscript is used to indicate that the parameters are determined or defined based on $\mathcal{L} = \sqrt{A}$. The parameter B was replaced by $Nu^0_{\sqrt{A}}$. In an earlier work of Yovanovich[4] on $Nu^0_{\sqrt{A}}$ for isothermal bodies of arbitrary shape at near zero Rayleigh number, the superiority of the square root of the body surface area to the classical body lengths was demonstrated as the values were shown to collapse into a relatively narrow range for various body shapes. Body shapes including elliptic disks, prolate spheroids, and right circular cylinders with aspect ratios ranging from 1 to 8 were examined in his study. The aspect ratio was defined as the ratio of the height to the width of the body. All reported diffusive limits lie in the range $3.180 \le Nu^0_{\sqrt{A}} \le 4.080$, and there is only a 28% difference between the minimum and maximum values corresponding to the hexagon and an elliptic disk with an aspect ratio of 8, respectively. More body shapes such as oblate spheroids, sphere, bisphere, and cubes in different orientations were examined in Ref. 6. The additional results lie in the range $3.342 \le Nu^0_{\sqrt{A}} \le 3.545$ with a maximum difference of only 6%. The minimum value corresponds to the thin oblate spheroid of 0.1 aspect ratio, and the maximum value corresponds to the sphere whose aspect ratio is 1.

The laminar heat transfer coefficient $C_{\sqrt{A}}$ in Eq. (4) is an empirical correlation coefficient, which was determined from the air data by means of a least-squares fit. Typical values of $C_{\sqrt{A}}$ range from 0.477 for a bisphere to 0.526 for a sphere.[4] Other $C_{\sqrt{A}}$ values of various body shapes examined in Ref. 6 are all bounded by the above range.

Yovanovich[5,6] was successful in collapsing the published heat transfer data into a narrow range by choosing the square root of the body surface area as the characteristic length over the range $0 \le Ra_{\sqrt{A}} < 10^8$. He proposed a single expression that is extremely simple and general for "rough" estimates with a percentage difference of approximately 8% over a wide range of body shapes and aspect ratios.

Although $\sqrt{A}$ was shown to be a superior characteristic length, and $Nu^0_{\sqrt{A}}$ was observed to be a weak function of body shapes, there is at present no theoretical basis that 1) demonstrates that $\sqrt{A}$ is the preferred characteristic length in laminar natural convection heat transfer and 2) explains why the laminar heat transfer coefficient $C_{\sqrt{A}}$ is relatively insensitive to body shapes and orientations.

In the following sections, the body-gravity function and, therefore, $C_{\sqrt{A}}$ are shown to be weak functions of body shapes and orientations over a wide range of aspect ratios. The $\sqrt{A}$ is deduced, based on the analysis, as the characteristic body length.

Analysis

Only the laminar part of heat transfer, as indicated by $CRa^{1/4}$ in the previous section, is of interest in the present study. Consider steady, laminar natural convection heat transfer from isothermal bodies to an extensive, quiescent fluid. The bodies are either two dimensional or axisymmetric and are free of pockets and horizontal planes. A section of the body surface and the coordinate system are shown in Fig. 1. By assuming that the boundary layers are thin, the usual set of

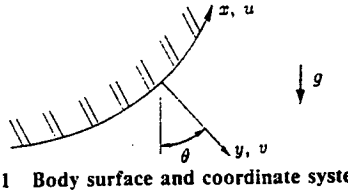

Fig. 1 Body surface and coordinate system.

dimensionless governing equations that describe laminar momentum and heat transfer in the fluid may be written as

$$\frac{\partial}{\partial x}\left(u\frac{P}{\mathcal{L}}\right)+\frac{\partial}{\partial y}\left(v\frac{P}{\mathcal{L}}\right)=0 \tag{5}$$

$$\frac{1}{Pr}\left[u\frac{\partial u}{\partial x}+v\frac{\partial u}{\partial y}\right]=\frac{\partial^2 u}{\partial y^2}+Ra_{\mathcal{L}}\,\Phi\sin\theta \tag{6}$$

$$u\frac{\partial\Phi}{\partial x}+v\frac{\partial\Phi}{\partial y}=\frac{\partial^2\Phi}{\partial y^2} \tag{7}$$

For two-dimensional bodies, the parameter $P/\mathcal{L}$ may be omitted from Eq. (5). For axisymmetric bodies, P is related to θ as will be seen later. An arbitrary length scale $\mathcal{L}$ and a velocity scale $\alpha/\mathcal{L}$ were used to nondimensionalize corresponding variables in the above equations.

The hydrodynamic and thermal boundary conditions associated with the above equations are

$$\text{at } y=0, \qquad u=v=0, \qquad \Phi=1 \tag{8a}$$

$$\text{as } y\to\infty, \qquad u\to 0, \qquad \Phi\to 0 \tag{8b}$$

$$\text{at } x=0, \qquad u=\Phi=0 \tag{8c}$$

The no-slip condition is used on the body, and the zero velocity condition is used at locations remote from the body where the fluid temperature is assumed to be uniform.

Solutions to the above set of laminar boundary-layer equations for $Pr\to\infty$ can be obtained by similarity methods as demonstrated by Acrivos[10] and Stewart.[11] A large Prandtl number not only allows one to neglect the convection terms on the left side of the momentum equation, Eq. (6), but also further ensures that the thermal boundary layer is thinner than the momentum boundary-layer thickness. It can be shown by integrating the resulting local Nusselt number expression over the surface area that the area-mean Nusselt number may be expressed as

$$Nu_{\mathcal{L}}=F_\infty G_{\mathcal{L}} Ra_{\mathcal{L}}^{1/4} \tag{9}$$

where the constant coefficient F_∞ is related to the outward normal surface temperature gradient with respect to the similarity variable and has a value of 0.670. The body-gravity function $G_{\mathcal{L}}$ is a geometric function that exclusively accounts for the effects of body shape and its orientation with respect to the direction of the gravity vector. It may be expressed in the form

$$G_{\mathcal{L}}=\left[\frac{1}{A}\int\!\!\int_A\left(\frac{P\sin\theta}{A/\mathcal{L}}\right)^{1/3}d\mathcal{A}\right]^{3/4} \tag{10}$$

This function can also be derived from the relationship obtained by the Raithby-Hollands approximate method,[12,13] which was developed by applying the integral method over the part of the boundary layer near the surface where both momentum and heat transfer due to convection are assumed negligible.

The above area-mean Nusselt number, Eq. (9), is derived for the limiting value as $Pr\to\infty$. In order to account for the Prandtl number effect, the coefficient F_∞ is replaced by a universal Prandtl number function $F(Pr)$ proposed by Churchill and Churchill[14] (also see Churchill and Thelen[15]). It is applicable for arbitrary body shapes and is given by

$$F(Pr)=\frac{0.670}{[1+(0.5/Pr)^{9/16}]^{4/9}} \tag{11}$$

Insofar as the analysis for thin, laminar boundary-layer heat transfer from a two-dimensional or axisymmetric body shape is concerned, the coefficient $C_{\mathcal{L}}$ can be evaluated from

$$C_{\mathcal{L}}=F(Pr)G_{\mathcal{L}} \tag{12}$$

and an arbitrary length scale $\mathcal{L}$ may be used as the characteristic length. However, in view of bringing together the $Nu_{\mathcal{L}}$ vs $Ra_{\mathcal{L}}$ plots for laminar natural convection heat transfer from various body shapes, a further investigation is required for the choice of the characteristic length.

Characteristic Length

Consider the body-gravity function given by Eq. (10). The numerator $P\sin\theta$ appearing in the integrand is the local perimeter weighted by the tangential component of the unit gravity vector. This length parameter, when multiplied by the thickness of the boundary layer, represents the local cross-sectional area of the thin boundary layer through which the effective buoyant force is induced upon the fluid. One option to nondimensionalize this parameter is to normalize it by its maximum value P_{max}. This leads to

$$\mathcal{L}=A/P_{max} \tag{13}$$

This length scale is sensitive to orientation. It is similar to the one proposed by Weber et al.,[3] who reported success in bringing closer together the laminar natural convection boundary-layer solutions for a number of bodies, most of which are also considered in the present investigation.

Another option is to choose the denominator of the integrand in Eq. (10) $A/\mathcal{L}$ to be the nondimensionalizing length scale for the local length parameter $P\sin\theta$. In this case, the denominator itself should be considered as the characteristic length, and it follows that $A/\mathcal{L}=\mathcal{L}$ or

$$\mathcal{L}=\sqrt{A} \tag{14}$$

Unlike the length scale defined by Eq. (13), this characteristic length is insensitive to orientation.

The $G_{\mathcal{L}}$ values with $\mathcal{L}$ specified by the classical body length L_c, A/P_{max}, and $\sqrt{A}$ are tabulated in Table 1; the data are obtained from Refs. 6 and 9. See Fig. 2 for schematics of the body shapes, dimensions, and orientations referred to in the table.

Table 1 shows that the values of the body-gravity function lie in the ranges $0.627 \le G_{L_c} \le 0.956$ with a maximum deviation of 53%, $0.613 \le G_{A/P_{max}} \le 0.956$ with a maximum deviation of 56%, and $0.768 \le G_{\sqrt{A}} \le 1.058$ with a maximum deviation of 38%. The minimum $G_{\mathcal{L}}$ values all correspond to the thin oblate spheroids with $a/b=0.1$. The maximum $G_{\mathcal{L}}$ values correspond to the vertical circular cylinders with hemispherical ends for $\mathcal{L}=L_c$ and A/P_{max}, and the flat square disks in orientation 2 for $\mathcal{L}=\sqrt{A}$. When thin, horizontal bodies, such as the thin oblate spheroid with $a/b=0.1$, short vertical cylinder with $L/D=0.1$, and flat square disk in orientation 3 are excluded, the above ranges become significantly narrower as the minimum values of $G_{\mathcal{L}}$ increase to 0.738, 0.805, and 0.928 for $\mathcal{L}=L_c$, A/P_{max}, and $\sqrt{A}$, respectively. These minimum values correspond to the bispheres for $\mathcal{L}=L_c$ and $\sqrt{A}$ and the oblate spheroid with $a/b=0.5$ for $\mathcal{L}=A/P_{max}$. Accordingly, the above maximum deviations in the $G_{\mathcal{L}}$ values become 30%, 19%, and 14% for $\mathcal{L}=L_c$, A/P_{max}, and $\sqrt{A}$, respectively.

In addition to the above findings, an interesting observation is made regarding the sensitivity of the characteristic length with respect to the orientation of the body. According to Weber et al.,[3] the first of three criteria for selecting a charac-

Table 1 Body-gravity functions obtained from experimental data[6,9] for various body shapes based on different characteristic length scales

Body shape	L_c, G_{L_c}	$G_{A/P_{max}}$	$G_{\sqrt{A}}$
Sphere	D, 0.887	0.887	1.023
Vertical bisphere	D, 0.738	0.877	0.928
Cylinder (L/D = 1)	(5.4)[a]	(1.1)	(5.4)
Axis-vertical	D, 0.797	0.882	0.967
Axis at 45 deg	D, 0.827	0.872	1.004
Axis-horizontal	D, 0.839	0.875	1.019
Cylinder (L/D = 0.1)	(31.6)	(43.8)	(31.6)
Axis-vertical	D, 0.713	0.628	0.772
Axis-horizontal	D, 0.939	0.903	1.016
Cylinder with hemi-spherical ends	(14.6)	(9.0)	(3.7)
Axis-vertical	H, 0.956	0.956	1.012
Axis-horizontal	D, 0.834	0.877	1.049
Spheroid (a/b = 1.93)	a, 0.841	0.934	1.012
Spheroid (a/b = 0.5)	b, 0.766	0.805	0.973
Spheroid (a/b = 0.1)	b, 0.627	0.613	0.768
Cube	(6.6)	(5.8)	(6.6)
Orientation 1	L, 0.760	0.841	0.951
Orientation 2	L, 0.791	0.836	0.990
Orientation 3	L, 0.811	0.884	1.014
Square disk	(27.9)	(46.0)	(27.9)
Orientation 1	L, 0.931	0.952	1.039
Orientation 2	L, 0.948	0.895	1.058
Orientation 3	L, 0.741	0.652	0.827

[a]Numbers in brackets represent maximum percentage differences in $G_{\mathcal{L}}$ values for the same body shape in different orientation.

teristic length was "the length would change for the same particle in different orientations." However, an examination reveals that A/P_{max}, which is sensitive to body orientations, is inferior to the other two characteristic lengths, which are insensitive to body orientations. Consider the values indicated in the brackets in Table 1. They represent the maximum percentage differences in $G_{\mathcal{L}}$ values incurred due to only the changes in orientation of fixed body shapes. Although the circular cylinder with $L/D = 0.1$ and the flat square disk show large differences between the maximum and minimum $G_{\mathcal{L}}$ values for any characteristic length, the differences are largest when $\mathcal{L} = A/P_{max}$ is used as the characteristic length, and they are in excess of 40% for both body shapes as indicated in the table.

Based on the above observation, $\sqrt{A}$ is clearly shown to be the superior choice of the characteristic length in narrowing the range of the values of the body-gravity function for the various bodies examined in Table 1. This characteristic length is identical to the one proposed by Yovanovich,[4] who demonstrated its superiority in his study of Nusselt numbers in the diffusive limit. In this limit as $Ra \to 0$, heat transfer is entirely due to conduction and, therefore, is independent of orientation. This allows one characteristic length $\sqrt{A}$ to be used throughout the diffusive and laminar regimes $0 \le Ra_{\sqrt{A}} < 10^8$. Other characteristic lengths, such as those summarized in Ref. 4, are examined also and are shown to be inferior to $\sqrt{A}$ in narrowing the ranges of $G_{\mathcal{L}}$ and, in turn, the resulting $Nu_{\mathcal{L}}$.

Body-Gravity Function

The expression of the area-mean Nusselt number, obtained as a result of the thin laminar boundary-layer analysis from the previous section, is summarized as

$$Nu_{\sqrt{A}} = F(Pr) G_{\sqrt{A}} Ra_{\sqrt{A}}^{1/4} \tag{15}$$

where $F(Pr)$ is given by Eq. (11), and $G_{\sqrt{A}}$ is obtained from Eq. (10) as

$$G_{\sqrt{A}} = \left[\frac{1}{A} \int\int_A \left(\frac{P \sin\theta}{\sqrt{A}} \right)^{1/3} d\mathcal{A} \right]^{3/4} \tag{16}$$

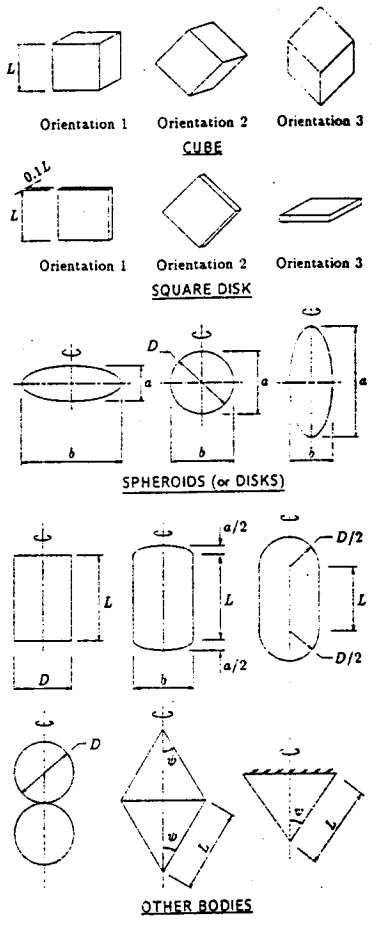

Fig. 2 Body shapes, dimensions, and orientations.

In addition to the above general expression for the body-gravity function, the following expressions are useful when a body shape under investigation consists of two or more distinctive body shapes in combination. As an example of such bodies, a cylinder with hemispherical ends can be considered as a combination of a cylinder with insulated ends and two hemispheres. When such bodies are placed in parallel with respect to the gravity vector, as in the case of a horizontal cylinder, the bodies are assumed not to be interfering and thus to be independent of each other. The area-mean average body-gravity function for such cases with N distinctive bodies can be obtained from

$$G_{\sqrt{A}} = \sum_{i=1}^{N} G_{\sqrt{A_i}} \tilde{A}_i^{7/8} \tag{17}$$

where $G_{\sqrt{A_i}}$ represents the body-gravity function for each separate body shape, and $\tilde{A}_i$ denotes the fraction of each body area in relation to the total surface area:

$$\tilde{A}_i = A_i/A \tag{18}$$

When a combination of N bodies are aligned in series with respect to the flow stream, as in the case of a vertical cylinder with hemispherical ends, the area-mean average body-gravity function for the combination can be obtained from

$$G_{\sqrt{A}} = \left[\sum_{i=1}^{N} G_{\sqrt{A_i}}^{4/3} \tilde{A}_i^{7/6} \right]^{3/4} \tag{19}$$

Also, when two-dimensional bodies, such as a vertical disk of an arbitrary shape as shown in Fig. 3, have a variable perimeter P as a function of x, the body-gravity function is

obtained by integrating the result that is evaluated for a differential surface with a width dz. It follows that

$$G_{\sqrt{A}} = \frac{2}{A^{7/8}} \int_0^{P_{max}/2} S(z)^{3/4}\, dz \tag{20}$$

where $S(z)$ denotes the flow distance from the leading edge to the trailing edge of the differential surface.

Equations (16–20) are used to evaluate the body-gravity function for various body shapes. They are compared with the experimental data[6,9] in Table 2. The values are shown to be in good agreement, except for the cases of thin body shapes and the cube in different orientations. In particular, the largest difference of 12.3% is observed for the thin oblate spheroid, and this will be discussed in a later section. Excluding the thin oblate spheroid, the differences for the remaining axisymmetric bodies included in the table are all less than 2%.

A further examination of the body-gravity function given by Eq. (16) reveals the qualitative behavior of the function that may explain why this function and, therefore, the area-mean Nusselt number are relatively insensitive to the geometry and orientation of body shapes. Consider axisymmetric bodies of an arbitrary shape that do not possess pockets and horizontal surfaces as shown in Fig. 4. Introducing r, $\sin\theta$ can be related to r from the relation

$$\sin\theta = \sqrt{1 - \left(\frac{dr}{dx}\right)^2} \tag{21}$$

This relationship can readily be rearranged and integrated over the surface to yield

$$\sum P_{\text{local max}} - \sum P_{\text{local min}} = \pi \iint_A \frac{\sqrt{1 - \sin^2\theta}}{P}\, d\mathcal{A} \tag{22}$$

where the left side represents the difference in the sum of local maximum and local minimum perimeters.

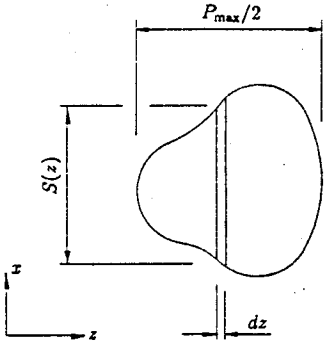

Fig. 3 Two-dimensional body with variable perimeter.

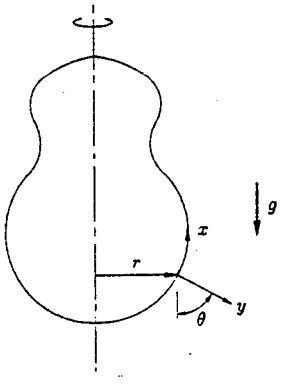

Fig. 4 Axisymmetric body.

If the bodies do not possess surface depressions, this equation can further be simplified as

$$P_{max} = \pi \iint_A \frac{\sqrt{1 - \sin^2\theta}}{P}\, d\mathcal{A} \tag{23}$$

Since the left sides of Eqs. (22) and (23) are finite for given bodies, the above expressions clearly illustrate the inverse relationship that exists between P and $\sin\theta$ over an area-integral. Recalling the body-gravity function given by Eq. (16) and its variable part of the integrand $P \sin\theta$, it may be stated for axisymmetric bodies that $G_{\sqrt{A}}$ is a weak function of body shape due to the repeated fractional powers appearing in its expression and to the effect of the inversely related constituents of the integrand over the area-integral.

Aspect Ratio

The body-gravity function given by Eq. (16) will be evaluated for various body shapes at different aspect ratios. A number of definitions were used in the past to define an aspect ratio of a given body. One of the most commonly used definitions would be the ratio of the vertical height to the width of a body. However, this definition becomes inconsistent and ambiguous in some cases in which a smooth transition of a body shape may not be properly reflected by the changes in the values of the aspect ratio. Consider a horizontal circular cylinder as an example. When the length of the cylinder is greater than the diameter, an aspect ratio may be defined as the diameter (height) divided by the length (width). But as the length becomes smaller than the diameter, the aspect ratio under the same definition becomes ambiguous because the diameter could also be used alternatively to represent the width of the body. The aspect ratio of the cylinder in the limit as the length becomes zero may be either infinite or unity, depending on the choice for the width of the body.

By considering the numerator of the integrand in Eq. (16), and by recalling that the equation is applicable for both two-dimensional and axisymmetric bodies, it becomes apparent that a definition of the aspect ratio should be related to the perimeter of the body. This also eliminates the previously observed ambiguity and ensures a smooth, continuous transition in the values of the aspect ratios corresponding to gradual changes in the shape of the body.

Possible options for the aspect ratio that satisfy the criteria observed above include ratios such as $\sqrt{A}/P_{max}$ and $\pi A/P_{max}^2$. However, while thin, flat bodies are perceived to have small or

Table 2 Comparison of body-gravity functions: analytical vs experimental

Body shape	γ	$G_{\sqrt{A}}$ Eq. (16)	$G_{\sqrt{A}}$ Exp.	% difference
Sphere	1.000	1.014	1.023	−0.9
Vertical bisphere	2.000	0.930	0.928	0.2
Cylinder ($L/D = 1$)				
Axis-horizontal	0.785	1.051	1.019	3.1
Cylinder ($L/D = 0.1$)				
Axis-horizontal	1.428	1.088	1.016	7.1
Cylinder with hemispherical ends				
Axis-vertical	2.000	0.994	1.012	−1.7
Axis-horizontal	0.611	1.038	1.049	−1.0
Spheroid ($a/b = 1.93$)	1.930	1.003	1.012	−0.9
Spheroid ($a/b = 0.5$)	0.500	0.954	0.973	−1.9
Spheroid ($a/b = 0.1$)	0.100	0.674	0.768	−12.3
Cube				
Orientation 2	0.920	1.080	0.990	9.1
Orientation 3	1.283	1.091	1.014	7.5
Square disk				
Orientation 2	1.467	1.118	1.058	5.6

zero aspect ratios in the limit, these definitions do not allow ratios to become smaller than fixed nonzero finite values. As an example, the aspect ratio defined by $\pi A/P_{max}^2$ for a flat, horizontal circular disk of zero thickness is 1/2. Moreover, the aspect ratio that involves the total surface area in its definition often results in complex implicit expressions that need to be evaluated in the course of computing $G_{\sqrt{A}}$.

In light of the above discussions, the following definition of the aspect ratio γ is proposed:

$$\gamma = \frac{H}{P_{max}/\pi} \tag{24}$$

A constant π is introduced dividing P_{max} such that γ becomes unity for spheres.

Case Studies and Discussions

In the following, the body-gravity function is examined for two-dimensional and axisymmetric bodies of various shapes in different orientations over a wide range of aspect ratios. For the schematic configurations and dimensions of the bodies, refer to Fig. 2. Expressions for the body-gravity function and the aspect ratio are obtained for each body shape. The subscript $\sqrt{A}$ is omitted for brevity, and new subscripts are used to distinguish the corresponding body shapes. The results are tabulated and plotted as a function of γ and compared with $G_{\sqrt{A}}$ obtained from the experimental data of other investigators.

Two-Dimensional Bodies

Vertical elliptic disks and circular and elliptic cylinders in vertical and horizontal orientations are examined as two-dimensional bodies. Although a cylinder has a finite volume and is thus a three-dimensional body, its body-gravity function can be obtained by using the two-dimensional analysis. Vertical flat plates are the limiting case of elliptic cylinders as their minor axes become zero. The ends of the cylinders in axis-vertical orientation are horizontal surfaces and therefore are excluded from the analysis by assuming that they are insulated. The corner effects around the edges of end surfaces of the horizontal cylinders are ignored.

Vertical Elliptic Disks

From Eq. (20), which is developed for two-dimensional bodies with variable P, one obtains

$$G_{ED} = 1.178\,\gamma^{-1/8} \tag{25}$$

where

$$\gamma = \pi a/2b \tag{26}$$

Vertical Elliptic Cylinders or Flat Plates—Ends Insulated

From Eq. (16),

$$G_{VC} = 1.154\gamma^{-1/8} \tag{27}$$

where

$$\gamma = \pi L/aI_1 \tag{28}$$

$$I_1 = \int_0^{\pi} \sqrt{1 - e^2\cos^2\vartheta}\, d\vartheta \tag{29}$$

$$e^2 = 1 - (b/a)^2 \tag{30}$$

For a flat plate, a becomes the width, $b = 0$, and $I_1 = 2$. Since G_{VC} is only a function of γ, it can be seen that the expression for the body-gravity function with respect to γ for a flat vertical plate is identical to G_{VC}. Note that the value of the coefficient of G_{VC} is only 2% smaller than that of G_{ED}.

Horizontal Elliptic Cylinders—Ends Insulated

It may be expressed from Eq. (16) that

$$G_{HC} = \left(\frac{2\pi I_2^6}{\gamma I_1^7}\right)^{1/8} \tag{31}$$

where

$$\gamma = \pi a/2L \tag{32}$$

$$I_2 = \int_0^{\pi} [\sin\vartheta(1 - e^2\cos^2\vartheta)]^{1/3}\, d\vartheta \tag{33}$$

and I_1 and e^2 are defined previously by Eqs. (29) and (30). Here, a is either the major axis when $a/b > 1$ or the minor axis when $a/b < 1$.

Horizontal circular cylinders correspond to the case where $a/b = 1$. For this case, I_1 becomes π and I_2 becomes 2.587. Then, the above expression for G_{HC} reduces to

$$G_{HC} = 0.943\gamma^{-1/8} \tag{34}$$

This is approximately 20% smaller than G_{VC} for a fixed value of γ. The difference between G_{HC} and G_{VC} diminishes as b/a becomes small. When b/a is equal to zero, G_{HC} becomes identical to G_{VC} and both horizontal and vertical cylinders become flat vertical plates.

The above expressions do not account for heat transfer through the end surfaces of the cylinders. The present analysis is invalid for horizontal surfaces due to the assumption of the thin boundary layer. Hence, it is not capable of dealing with the horizontal end surfaces of the vertical cylinders. In the case of a horizontal cylinder, however, the effects of the end surfaces may be accounted for by treating the end surfaces as isolated vertical disks in a parallel combination with the cylinder as follows.

Horizontal Elliptic Cylinders—Ends Included

The body-gravity function for horizontal elliptic and circular cylinders, where all the surfaces are participating in heat transfer, may be obtained from Eq. (17). In terms of the above G_{HC} and G_{ED}, it leads to

$$G_{HC\,+\,ED} = G_{HC}\bar{A}_{HC}^{7/8} + G_{ED}\bar{A}_{ED}^{7/8} \tag{35}$$

where the subscript $HC + ED$ represents the combined effect of the horizontal cylinders and the vertical elliptic disks of the same b/a ratios.

The aspect ratio of the horizontal elliptic cylinders is given by

$$\gamma = \frac{\pi a}{2(L + b)} \tag{36}$$

and G_{HC} and G_{ED} are given by Eqs. (31) and (25), respectively. The aspect ratios defined by Eqs. (32) and (26) are given exclusively for G_{HC} and G_{ED}. It is to be noted therefore that, in evaluating G_{HC} and G_{ED} in Eq. (35) for $G_{HC\,+\,ED}$, both aspect ratios have to be modified in relation to the above γ.

Axisymmetric Bodies

Spheroids, vertical cylinders with hemispheroidal ends, and vertical double cones base-to-base are examined as axisymmetric bodies.

Spheroids

From Eq. (16), it can be obtained that

$$G_{SP} = \left(\frac{2\pi\mathcal{I}_2^6}{\gamma\mathcal{I}_1^7}\right)^{1/8} \tag{37}$$

where

$$\gamma = a/b \tag{38}$$

$$\mathfrak{I}_1 = 2\int_0^1 \sqrt{1-e^2t^2}\,dt \tag{39}$$

$$\mathfrak{I}_2 = 2\int_0^1 [(1-t^2)(1-e^2t^2)]^{1/3}\,dt \tag{40}$$

Notice the striking similarity that exists between the expressions of G_{SP} given above and G_{HC} given by Eq. (31).

Explicit expressions for $\mathfrak{I}_1$ are available. For prolate spheroids where $e^2 > 0$,

$$\mathfrak{I}_1 = \sqrt{1-e^2} + \frac{\sin^{-1} e}{e} \tag{41}$$

For oblate spheroids where $e^2 < 0$, or $\epsilon^2 = -e^2 > 0$,

$$\mathfrak{I}_1 = \sqrt{1+\epsilon^2} + \frac{\ln(\epsilon + \sqrt{1+\epsilon^2})}{\epsilon} \tag{42}$$

And for spheres where $e^2 = 0$, $\mathfrak{I}_1$ becomes 2 and $\mathfrak{I}_2$ becomes 1.684, resulting in a constant for G_{SP} as

$$G_{SP} = 1.014 \tag{43}$$

Vertical Circular Cylinders with Hemispheroidal Ends

This case is an in-line combination of a vertical circular cylinder and hemispheroids whose horizontal diameter b is equal to the diameter of the circular cylinder. From Eq. (19), the body-gravity function can be obtained as

$$G_{VC+SP} = (G_{VC}^{4/3}\tilde{A}_{VC}^{7/6} + G_{SP}^{4/3}\tilde{A}_{SP}^{7/6})^{3/4} \tag{44}$$

where G_{VC} is given by Eq. (27) and G_{SP} is given by Eq. (37). Again, the parameters on the right side of the above equation need to be evaluated in terms of γ defined by

$$\gamma = (a+L)/b \tag{45}$$

Vertical Double Cones Base-to-Base

Evaluating Eq. (19) for an in-line combination of two identical cones,

$$G_{DC} = \frac{G_{SC}}{2^{1/8}} = 1.121\left[\frac{\gamma^2}{(1+\gamma^2)^{3/2}}\right]^{1/8} \tag{46}$$

where

$$\gamma = \cot\psi \tag{47}$$

and G_{SC} denotes the body-gravity function obtained for a single vertical cone with end surface insulated:

$$G_{SC} = 1.222\,(\cos^2\psi\,\sin\psi)^{1/8} \tag{48}$$

In addition to the body shapes described above, the case of horizontal circular cylinders with hemispherical ends is included. This is neither a two-dimensional nor axisymmetric body, but a mixture of two bodies in a parallel combination. Therefore, from Eq. (17), one obtains

$$G_{HC+SP} = G_{HC}\tilde{A}_{HC}^{7/8} + G_{SP}\tilde{A}_{SP}^{7/8} \tag{49}$$

where G_{HC} for horizontal circular cylinders is given by Eq. (31), and G_{SP} for spheres is given by Eq. (43). The aspect ratio is given by

$$\gamma = \left[1 + \frac{2L}{\pi D}\right]^{-1} \tag{50}$$

The two-dimensional body-gravity functions for the vertical cylinders, elliptic disks, and horizontal cylinders with $a/b = 1/2, 1, 2$ are computed with respect to γ. They are tabulated in Table 3 and plotted in Fig. 5. The maximum value of γ of a horizontal elliptic cylinder with a fixed a/b occurs when the cylinder becomes a disk at $L = 0$. As shown in the figure, the body-gravity function of the cylinder becomes identical to that of an isolated disk as L approaches zero, or equivalently, as γ approaches its maximum value as it should. Also, the experimental data from Table 2 for the case of horizontal circular cylinders ($a/b = 1$) are included in the figure as discrete points.

The body-gravity functions for the cases of the axisymmetric bodies and the horizontal cylinder with hemispherical ends are also tabulated in Table 3 and plotted in Fig. 6. Two cases of vertical cylinders, one with thin semioblate spheroidal ends where $a/b = 0.2$ and another with hemispherical ends where $a/b = 1$ are included in the table and the figure. The experimental data from Table 2 for the spheroids and circular cylinder with hemispherical ends are compared in the figure. An excellent agreement is revealed, except for the case of the thin oblate spheroid.

As mentioned throughout this study, the present analysis is developed under the assumption of thin boundary layer. It is insufficient in predicting heat transfer from bodies of small and large aspect ratios. At large aspect ratios, both two-dimensional and axisymmetric bodies become vertically elongated shapes. In the limit as $\gamma \to \infty$ with $Ra_{\sqrt{A}}$ fixed, the bodies become infinitely long and thin and, hence, the assumption of thin boundary layer becomes invalid. A number of publications exist in the literature dealing with this type of problem.[16-18]

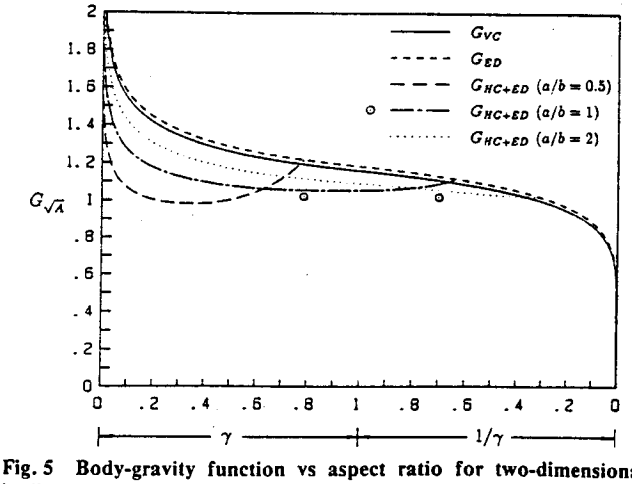

Fig. 5 Body-gravity function vs aspect ratio for two-dimensional bodies.

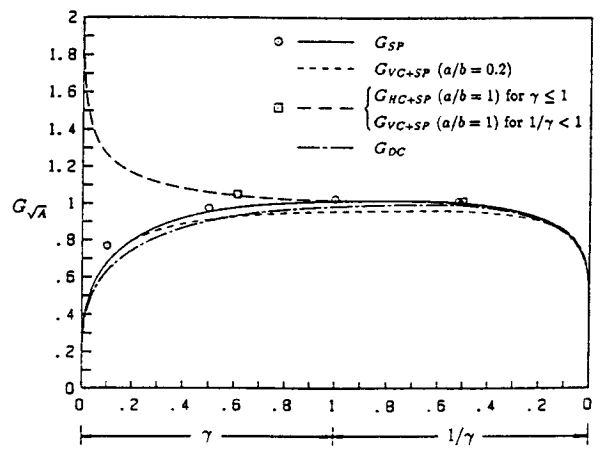

Fig. 6 Body-gravity function vs aspect ratio for axisymmetric bodies and horizontal circular cylinder with hemispherical ends.

Table 3 Body-gravity functions for various body shapes: analytical results

		Two-dimensional bodies					Axisymmetric bodies			
				G_{HC+ED}					G_{VC+SP}	
γ	$1/\gamma$	G_{VC}	G_{ED}	$(a/b=0.5)$	$(a/b=1)$	$(a/b=2)$	G_{DC}	G_{SP}	$(a/b=0.2)$	G^a
0.1	—	1.539	1.571	1.063	1.267	1.416	0.629	0.674	—	1.263
0.2	—	1.411	1.440	1.000	1.172	1.302	0.744	0.798	0.798	1.164
0.3	—	1.341	1.369	0.981	1.124	1.240	0.816	0.872	0.853	1.112
0.4	—	1.294	1.321	0.984	1.094	1.199	0.867	0.921	0.889	1.079
0.5	—	1.258	1.284	1.005	1.075	1.169	0.904	0.954	0.912	1.056
0.6	—	1.230	1.255	1.046	1.062	1.146	0.931	0.977	0.928	1.040
0.7	—	1.206	1.231	1.117	1.054	1.127	0.951	0.992	0.940	1.028
0.8	—	1.186	1.211	—	1.050	1.111	0.966	1.003	0.947	1.020
0.9	—	1.169	1.193	—	1.049	1.098	0.977	1.009	0.953	1.016
1.0	—	1.154	1.178	—	1.051	1.086	0.984	1.014	0.957	1.014
—	0.9	1.139	1.162	—	1.056	1.075	0.990	1.016	0.959	1.014
—	0.8	1.122	1.145	—	1.066	1.064	0.993	1.017	0.961	1.013
—	0.7	1.104	1.126	—	1.088	1.052	0.995	1.015	0.961	1.010
—	0.6	1.082	1.105	—	—	1.040	0.993	1.010	0.959	1.004
—	0.5	1.058	1.080	—	—	1.028	0.986	1.001	0.955	0.994
—	0.4	1.029	1.050	—	—	1.020	0.972	0.985	0.946	0.980
—	0.3	0.993	1.013	—	—	—	0.949	0.961	0.931	0.957
—	0.2	0.944	0.963	—	—	—	0.910	0.922	0.903	0.921
—	0.1	0.865	0.883	—	—	—	0.839	0.850	0.846	0.855

[a]Circular cylinder with hemispherical ends; axis-horizontal for $\gamma \leq 1$ and axis-vertical for $1/\gamma < 1$.

On the other hand, when $\gamma \to 0$ with $Ra_{\sqrt{A}}$ fixed, two-dimensional bodies become horizontally long and thin, and axisymmetric bodies become horizontal, flat circular disks. Horizontally long and thin bodies have zero vertical flow distance and, thus entirely owing the boundary-layer assumption, the boundary-layer thickness becomes zero, which, in turn, results in infinite heat flow rates.

One can also obtain an infinitely small aspect ratio by increasing the horizontal length without changing the vertical height of two-dimensional bodies. The vertical flow distance from the leading stagnation point to the trailing stagnation point of the body is maintained, and the thin boundary-layer assumption may still be valid. In this case, however, $Ra_{\sqrt{A}}$ increases due to the larger surface area, and the analysis predicts infinite, average heat-transfer rates not because of the zero boundary-layer thickness but solely because of the choice of the characteristic length $\sqrt{A}$, which also becomes infinitely large in the limit. In either case of the above situations, the body-gravity function plotted in Fig. 5 consistently reflects the correct behavior of the analysis as $\gamma \to 0$.

Consider a horizontally flat circular disk, which all axisymmetric bodies become as $\gamma \to 0$. The present analysis predicts zero laminar convection heat transfer due to zero driving force along the body surface. In an actual situation, there will be isotherms forming in the vicinity of the disk as a result of pure diffusion at first. These isotherms have oblate spheroidal shapes and will induce driving forces on the fluid along the contour of the spheroidal surfaces. This induced convective heat transfer is not accounted for in the present thin boundary-layer analysis. Consequently, the current body-gravity function results in lower predictions when axisymmetrical bodies of small aspect ratios are examined, as seen in Table 2 and Fig. 6 for the case of the thin oblate spheroid.

Summary and Conclusions

1) A new form of the body-gravity function $G_{\mathcal{L}}$, which describes the dependency of the area-mean laminar Nusselt number on body shape and orientation, has been presented for two-dimensional and axisymmetric bodies.

2) Based on the new form of the body-gravity function, $\sqrt{A}$ is obtained as a characteristic length, and it was demonstrated that $\sqrt{A}$ is superior to other length scales.

3) It was explained for axisymmetric bodies, and demonstrated for various body shapes that the body-gravity function based on $\mathcal{L} = \sqrt{A}$ is fairly insensitive to body shapes and orientations for the range $0.2 \leq \gamma \leq 5$ where γ is the aspect ratio defined by Eq. (24).

Acknowledgments

The authors wish to acknowledge the financial support of the Natural Sciences and Engineering Research Council of Canada under Grant A7455. The financial support of Shiraz University, Shiraz, Iran for K. Jafarpur is also acknowledged.

References

[1]Sparrow, E. M., and Ansari, M. A., "A Refutation of King's Rule for Multi-Dimensional External Natural Convection," *International Journal of Heat Mass Transfer*, Vol. 26, No. 26, 1983, pp. 1357–1364.

[2]Sparrow, E. M., and Stretton, A. J., "Natural Convection From Variously Oriented Cubes and From Other Bodies of Unity Aspect Ratio," *International Journal of Heat Mass Transfer*, Vol. 28, No. 4, 1985, pp. 741–752.

[3]Weber, M. E., Astrauskas, P., and Petsalis, S., "Natural Convection Mass Transfer to Nonspherical Objects at High Rayleigh Numbers," *The Canadian Journal of Chemical Engineering*, Vol. 62, 1984, pp. 68–72.

[4]Yovanovich, M. M., "New Nusselt and Sherwood Numbers for Arbitrary Isopotential Bodies at Near Zero Peclet and Rayleigh Numbers," AIAA Paper 87-1643, June 1987.

[5]Yovanovich, M. M., "Natural Convection from Isothermal Spheroids in the Conductive to Laminar Flow Regimes," AIAA Paper 87-1587, June 1987.

[6]Yovanovich, M. M., "On the Effect of Shape, Aspect Ratio and Orientation Upon Natural Convection From Isothermal Bodies of Complex Shape," *Convective Transport*, ASME HTD-Vol. 82, edited by Y. Jaluria, R. S. Figliola, and M. Kaviany, American Society of Mechanical Engineers, New York, Dec. 1987, pp. 121–129.

[7]Churchill, S. W., and Chu, H. H. S., "Correlating Equations for Laminar and Turbulent Free Convection From A Vertical Plate," *International Journal of Heat Mass Transfer*, Vol. 18, 1975, pp. 1323–1329.

[8]Raithby, G. D., and Hollands, K. G. T., *Handbook of Heat Transfer*, 2nd ed., edited by W. M. Rohsenow, J. P. Hartnett, and E. N. Ganic, McGraw-Hill, New York, 1985, Chap. 6.

[9]Hassani, A. V., "An Investigation of Free Convection Heat Transfer from Bodies of Arbitrary Shape," Ph.D. Thesis, Dept. of Mechanical Engineering, Univ. of Waterloo, Waterloo, Ontario, Canada, 1987.

[10]Acrivos, A., "A Theoretical Analysis of Laminar Natural Convection Heat Transfer to Non-Newtonian Fluids," *AIChE Journal*, Vol. 6, 1960, pp. 584–590.

[11]Stewart, W. E., "Asymptotic Calculation of Free Convection in Laminar Three-Dimensional Systems," *International Journal of Heat Mass Transfer*, Vol. 14, 1971, pp. 1013–1031.

[12]Raithby G. D., and Hollands, K. G. T., "A General Method of Obtaining Approximate Solutions to Laminar and Turbulent Free Convection Problems," *Advances in Heat Transfer*, Vol. 11, Academic, New York, 1975.

[13]Raithby, G. D., and Hollands, K. G. T., "Analysis of Heat Transfer By Natural Convection (or Film Condensation) For Three Dimensional Flows," *Sixth International Heat Transfer Conference*, Toronto, Canada, Hemisphere, Washington, DC, Vol. 2, Aug. 1978, pp. 187–192.

[14]Churchill, S. W., and Churchill, R. U., "A Comprehensive Correlating Equation for Heat and Component Transfer by Free Convection," *AIChE Journal*, Vol. 21, 1975, pp. 604–606.

[15]Churchill, S. W., and Thelen, H. J., "Eine allgemeine Korrelationsgleichung für den Wärme- und Stoffübergang bei freier Konvektion," *Chemical Engineering Technology*, Vol. 47, 1975, pp. 45.

[16]Cebeci, T., and Na, T. U., "Laminar Free-Convection Heat Transfer From a Needle," *The Physics of Fluids*, Vol. 12, No. 2, 1969, pp: 463–465.

[17]Narain, J. P., and Uberoi, M. S., "Laminar Free Convection From Vertical Thin Needles," *The Physics of Fluids*, Vol. 15, No. 5, 1972, pp. 928, 929.

[18]Raithby, G. D., and Hollands, K. G. T., "Free Convection Heat Transfer From Vertical Needles," *Journal of Heat Transfer, Transactions of ASME*, Series C, Vol. 98, 1976, pp. 522, 523.